

# Fluid-structure coupling analysis and simulation of viscosity effect on Coriolis mass flowmeter

\*Luo Rongmo, and Wu Jian

National Metrology Centre, A\*STAR, 1 Science Park Drive, Singapore 118221.

\*Corresponding author: [luo\\_rongmo@nmc.a-star.edu.sg](mailto:luo_rongmo@nmc.a-star.edu.sg)

## Abstract

Coriolis mass flowmeters (CMFs) are increasingly used in the oil and gas industry with feature of directly measuring mass flow rate. The performance of CMFs influenced by on-line viscosity still needs further study. A computational fluid dynamics model of U-shape CMF was developed. The simulation results were evaluated in terms of the natural frequency of the vibrating system and the corresponding phase difference between the motions of the sensing points symmetrically located on the measuring tube. The simulations were conducted on comparison between water and viscous liquid with flow rates spanning the laminar and turbulent regions. The effects of viscosity on mass flow measurement by CMFs are discussed in details. The findings in the simulations can be used for further compensation of deviation due to viscosity effects.

**Keywords:** Coriolis mass flowmeter, Fluid-structure interaction, High viscosity, Deviation, Mass flow rate

## 1. Introduction

Coriolis mass-flow measurement is used in a huge range of industry sectors, including pharmaceuticals, chemicals and petrochemicals, oil and gas, and food. Although a Coriolis mass flow meter (CMF) is independent of flow profile or installation effects, it may be dependent on the Reynolds number ( $Re$ ) of the mean flow. The measurement deviation at low  $Re$  has significant importance in the metering of highly viscous fluids. Several laboratory and field measurements with certain devices clearly indicate that there can be a shift in the meter calibration factor at viscous liquid (Henry, Tombs et al. 2006, Kumar and Anklin 2011).

The flow measurement industry is one such example where application of these numerical tools is helping to improve product quality and to find innovative solutions. In many flow measurement devices, especially a CMF, fluid-structure interaction (FSI), i.e. where computational structural mechanics (CSM) and computational fluid dynamics (CFD) need to be coupled, related problems are often encountered and a complete understanding of physical phenomena occurring in devices becomes vital (Bobovnik, Mole et al. 2005, Mole, Bobovnik et al. 2008). As far as CMFs are concerned, there are a few attempts to simulate a CMF using coupled FSI approach (Mole, Bobovnik et al. 2008, Kumar and Anklin 2011).

In this paper, a three-dimensional coupled fluid-structure numerical model of a U-shape Coriolis flowmeter is presented. The excitation force has been complemented to address properly the forced vibration conditions of CMF, and then the CFD model is employed for the CMF operating under inflow fluid conditions with different viscosity. Results from coupled fluid-structure numerical simulations mainly for varied viscosity are presented. With the help of these simulations the fluid dynamic effect responsible for the meter deviation at different viscosity can be understood, and better resemblance can be achieved between the numerical model simulation and the true operation of the CMFs.

## 2. MATHEMATICAL MODELS

The fluid-conveying measuring sensor tube in the Coriolis mass flowmeter is maintained to vibrate periodically at its natural frequency under impulsively forced vibration conditions (resonance). Mass flow is usually measured as the time or phase difference between the motion of two sensing points ( $S_1$  and  $S_2$ ) on the tube, which are positioned symmetrically along the tube length. However, the distortion of symmetry of the no-flow drive mode is resulted from the interaction between the motion of the tube and the fluid flow due to the CMF's inertial force field, where the straight measuring tube is clamped at both ends and vibrating at its first natural frequency. This section presents the governing equations and corresponding general boundary/initial conditions which we have used in the present simulations.

### 2.1 Fluid domain

The conservation equations of mass and momentum are written in the integral form for the three-dimensional spatial distribution and time range ( $t > 0$ ) of fluid flow as

$$\frac{\partial}{\partial t} \int_{\Omega_F} \rho_F d\Omega + \int_{\Gamma_F} (\mathbf{V}_F - \mathbf{V}_s) \cdot \mathbf{n} d\Gamma = 0 \quad (1)$$

$$\frac{\partial}{\partial t} \int_{\Omega_F} \rho_F \mathbf{V}_F d\Omega + \int_{\Gamma_F} \rho_F \mathbf{V}_F (\mathbf{V}_F - \mathbf{V}_s) \cdot \mathbf{n} d\Gamma = \int_{\Gamma_F} \boldsymbol{\sigma}_F \cdot \mathbf{n} d\Gamma + \int_{\Omega_F} \mathbf{f}_F d\Omega \quad (2)$$

where movement of fluid flow with the density  $\rho_F(x, t)$  and the velocity  $V_F(x, t)$  in the domain  $\Omega_F (x \in \Omega_F)$  are influenced by the motion of a surrounding boundary velocity  $v_s$ ,  $\Gamma$  denotes the surface-area vector. The vector  $\mathbf{f}_F(x, t)$  in the momentum equation (2) is the volume forces acting inside the domain  $\Omega_F$ , and  $\boldsymbol{\sigma}_F(x, t)$  is the resulting tensor.

The respective boundary conditions can be written as

$$\begin{aligned} \mathbf{V}_F(x, t) &= \mathbf{V}_{\text{inflow}}, \quad x \in \Gamma_{\text{inflow}}, \\ p_F(x, t) &= p_{\text{outflow}}, \quad x \in \Gamma_{\text{outflow}}, \\ \mathbf{V}_F(x, t) &= v_s(x, t), \quad x \in \Gamma_{\text{tube}}^m(t), \\ \mathbf{V}_F(x, t) &= 0, \quad x \in \Gamma_{\text{tube}}^{\text{in}}(t), \quad x \in \Gamma_{\text{tube}}^{\text{out}}(t), \end{aligned} \quad (3)$$

where  $\mathbf{V}_{\text{inflow}}$  is the inflow fluid velocity,  $\Gamma$  is the fluid boundary,  $p_{\text{outflow}}$  is the absolute fluid pressure at fluid outflow, and  $v_s(x, t)$  is the velocity of the measuring tube surface.

### 2.2 Structure domain

The conservation of momentum principles is utilized for the three-dimensional spatial distribution ( $x \in \Omega_s$ ) and time evolution ( $t > 0$ ) of the structural response, where the respective equation of motion can be derived by Hamilton's variation principle,

$$\int_{t_1}^{t_2} \delta(W_p - W_k) dt = 0 \quad (4)$$

where  $W_p$  and  $W_k$  are the total potential energy and the total kinetic energy of the moving solid structure, respectively. The detailed expressions for them are defined as (Mole, Bobovnik et al. 2008),

$$W_p = \frac{1}{2} \int_{\Omega_s} \boldsymbol{\sigma}_s : \boldsymbol{\varepsilon}_s d\Omega - \int_{\Gamma_s} \mathbf{P}_s \cdot \mathbf{u}_s d\Gamma - \mathbf{F} \cdot \mathbf{r}_p \quad (5)$$

$$W_k = \frac{1}{2} \int_{\Omega_s} \rho_s (\mathbf{v}_s \cdot \mathbf{v}_s) d\Omega \quad (6)$$

where the surface tractions  $\mathbf{P}_s(x,t)$  acting upon the moving shell boundary through the respective displacement field  $\mathbf{u}_s(x,t)$ , and the concentrated force  $\mathbf{F}(t)$  at point P, where the forced vibration is generated.  $\varepsilon_s(x,t)$  and  $\sigma_s(x,t)$  are the strain and the stress tensor in the shell structure, and  $\mathbf{r}_p$  is the position vector of point P where the force  $\mathbf{F}$  is applied.  $\rho_s(x,t)$  is the structure material density and  $\mathbf{v}_s(x,t)$  is the structure velocity field.

At  $t=0$ , the initial velocity and acceleration fields,  $\mathbf{v}_s(x,0)$  and  $\mathbf{a}_s(x,0)$  must be given, and  $\sigma_s(x,0) = \varepsilon_s(x,0) = 0$ . At  $t > 0$ ,

$$\begin{aligned}\mathbf{u}_s(x,t) &= 0, \quad x \in \Gamma_{\text{tube}}^u, \\ \boldsymbol{\sigma}_s(x,t) \cdot \mathbf{n}(x,t) &= \mathbf{P}_s(x,t), \quad x \in \Gamma_{\text{tube}}^u(t), \\ \mathbf{F}(t) &= (\mathbf{F}(t), 0, 0), \quad x = x_p\end{aligned}\quad (7)$$

For the structural-side boundary conditions, the sensing tube was fixed at both ends. In order to simulate the tube exciter, a periodic or harmonic force was applied at the center of tube point P. The first frequency of the sensing tube (the drive frequency of the meter) is equal to the frequency of the oscillating force. A periodic force was applied at the centre Point P to oscillate the pipe in the x-direction,

$$\mathbf{F}(t) = (F_0 \sin(2\pi n f_d \Delta t), 0, 0) \quad (8)$$

where  $\Delta t$  is the integration time step,  $f_d$  denotes the drive frequency, and  $F_0$  represents the amplitude of the periodic force.

### 2.3 Method of analysis

The present simulation uses the ANSYS Workbench framework employing DesignModeler, SIMULATION, ANSYS, CFX Mesh and CFX solver. The pipe is created in DesignModeler, with the structural and fluid domain representing the tube wall and the fluid inside the tube. SIMULATION and CFX Mesh are used to mesh the solid and fluid domain, respectively.

To determine the investigated tube's natural frequency, a modal analysis of the solid domain is conducted in ANSYS. The determined natural frequency is used to calculate the excitation force at point P. And then a dynamic response analysis for the solid domain is performed based on the linear elastic theory, where the deformations of the sense tube are assumed to be small. And it can determine the time step for FSI analysis.

To obtain the initial conditions for the transient fluid analysis, a steady state analysis is carried out in CFX over the fluid domain.

The two steady state analyses are employed for the transient analysis of the fluid domain. The FSI simulations are carried out within CFX (ANSYS v13.0).

During the information transferring, both the kinematic and dynamic constraints are set for the FSI interface,

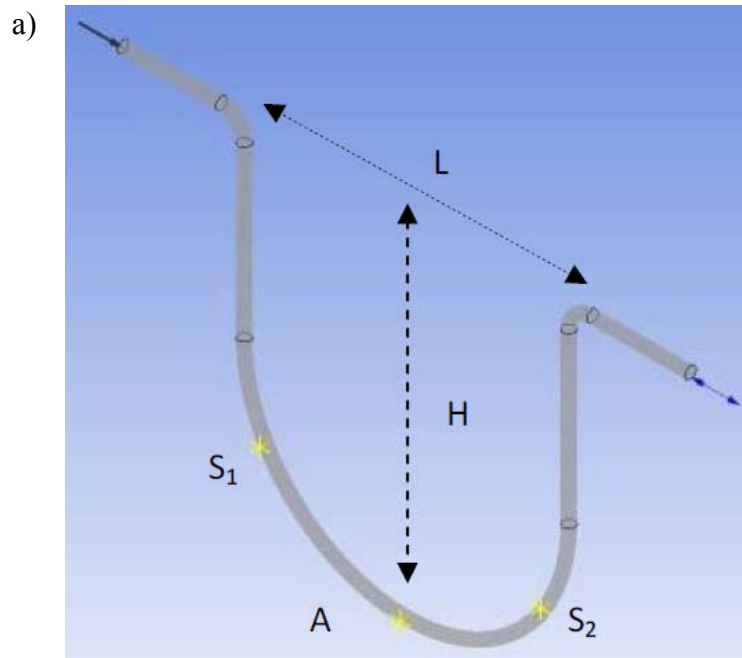
$$\begin{aligned}\mathbf{V}_F(x, t_n)|_F &= \mathbf{V}_F(x, t_n)|_s \\ \mathbf{u}_s(x, t_n)|_s &= \mathbf{u}_s(x, t_n)|_F \\ F_j^{\text{FSI}} &= \int (p\delta_{ij} + \sigma_{ij})d\Gamma_i^{\text{FSI}}\end{aligned}\quad (9)$$

where  $F_j^{\text{FSI}}$  denotes the total force vector from the CFX solver to the structural solver, and  $\sigma_{ij}$  includes the viscous and turbulent part of the momentum tensors. On the other hand, structural displacements  $\mathbf{u}_s(x, t_n)$  are transferred from the structure to the fluid in order to fulfill kinematic constraints.

### 3. RESULTS AND DISCUSSION

The analyzed U-shape CMF, with geometry as presented in Fig. 1(a), is characterized by the length of span  $L=0.4$  m and height of CMF  $H=0.38$  m, and a cross-section geometry which is determined by the internal diameter  $D=0.0254$  m and wall thickness  $\delta=1/40D$ . The distance between the symmetrically positioned sensing points  $S_1$  and  $S_2$  is equal to  $L_s=0.36$  m. The specifications used for the simulations in this work are shown in Table 1.

As the structure has multiple degrees of freedom, the structure will vibrate in a different manner at different natural frequencies without any application of external forces. Looking at all the deformations of the respective frequencies, in order for resonance to occur, the driver has to impose a driving force at the natural frequency  $f_d = 73.853$  Hz, as shown in Fig. 1(b).



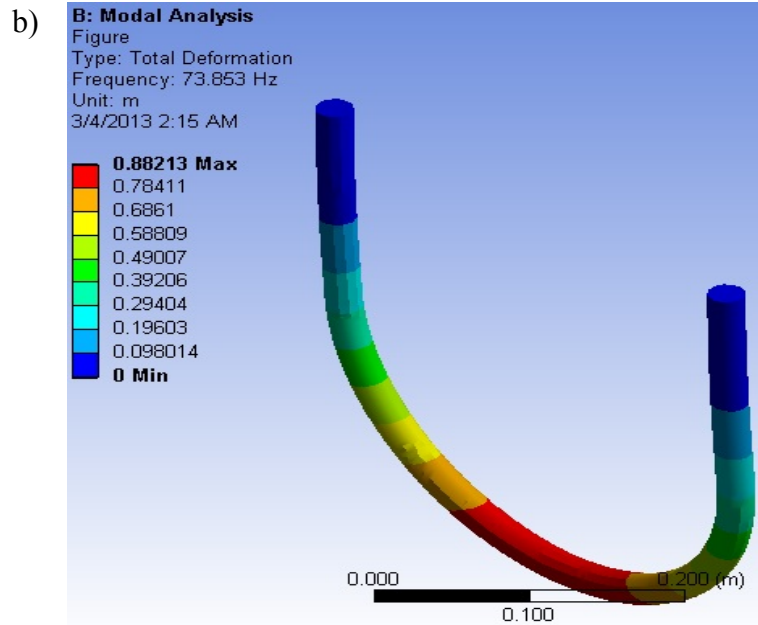


**Figure 1. a) Sensor points, and geometry of the U-shape CMF, and b) modal analysis for natural frequency at 73.853Hz.**

**Table 1. Input parameters for modeling and simulations**

Specifications	Dimensions and Values
Internal diameter of tube (D)	0.0254 m
Thickness of tube	1/40D
Material	Stainless steel 316
Poisson ratio	0.3
Young's modulus	1.93E+11 Pa
Density of stainless steel 316 tube	8000kg/m <sup>3</sup>
Viscosity of liquid fluid	1 - 500 cSt
Density of water	998.2kg/ m <sup>3</sup>
Tested fluid's velocities	2m/s - 20m/s
Number of time steps	100

Through the simulation, the time shift can be gained between the two sensor points  $S_1$  and  $S_2$ , as shown in Fig 2. The blue curve plots the displacement at monitor point 1, where the excitation force is applied. The red curve plots the displacement at the sensor point  $S_1$  which is near the inlet. The green curve plots the mesh displacement at the sensor point 2 which is near the outlet.

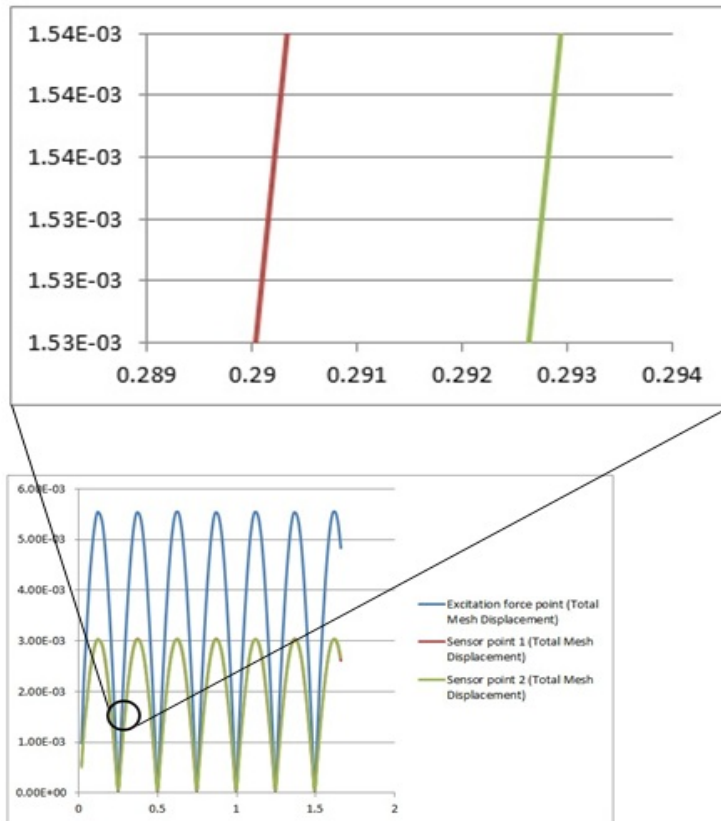


**Figure 2. Example result of time difference between sensors  $S_1$  and  $S_2$ .**

The developed FSI model are employed to investigate the effect on fluid viscosity on the performance of the U-shape CMF, including viscosities 50 cSt, 100 cSt, 180 cSt and 500 cSt. The results of time shift  $\delta t$  between sensors  $S_1$  and  $S_2$  for the various viscosities are shown in Fig 3. The time shift increases with the nominal flow velocity, and the drift from the result of water ( $\mu=1$  cSt) of time shift becomes obvious at high velocity.

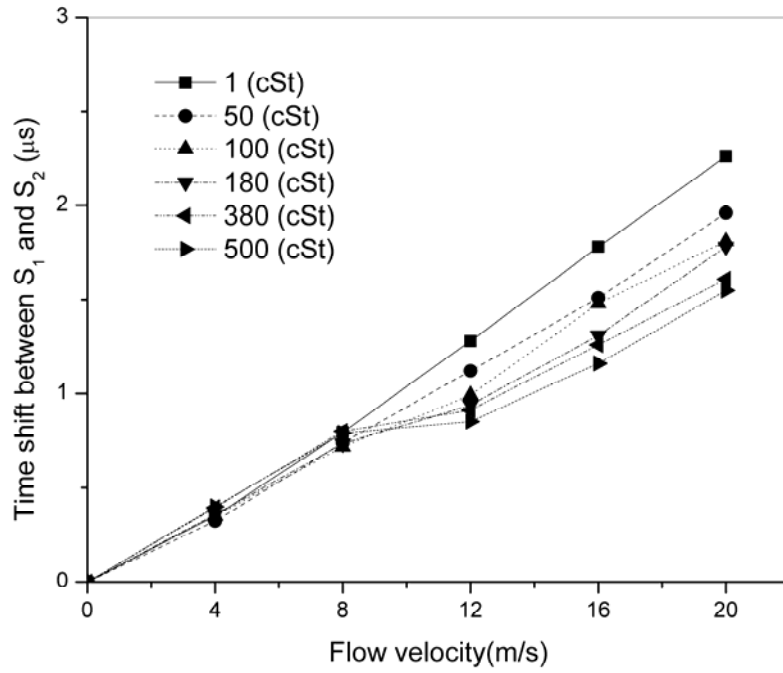


Figure 3. Time shift between sensors  $S_1$  and  $S_2$  against fluid viscosity.

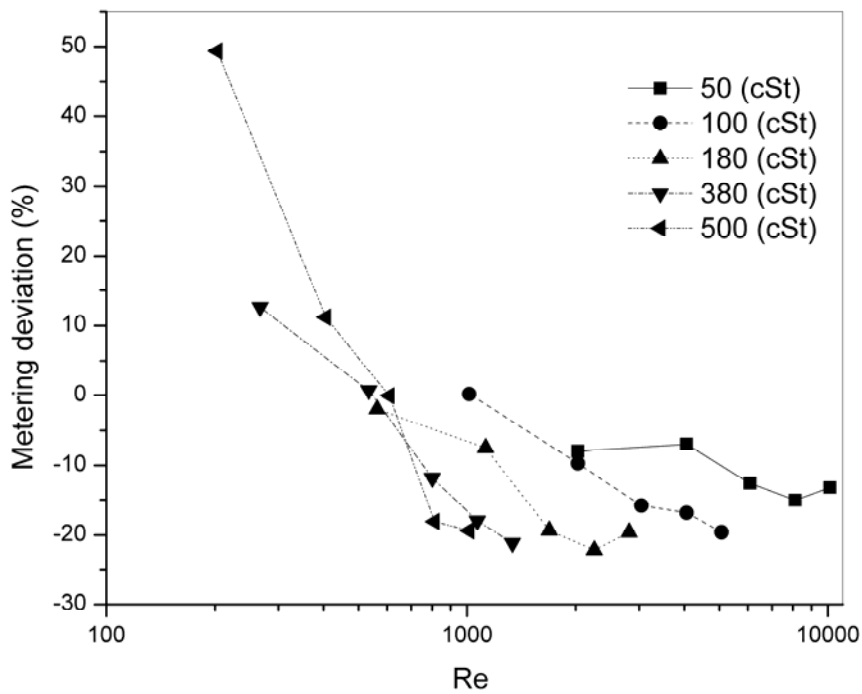


Figure 4. Deviation to water metering of phase difference for different fluid's viscosities.

Since the mass flow rate  $\dot{m}$  of a CMF can be calculated by  $\dot{m} = K_f \delta t$ , where  $K_f$  is the meter factor, and  $\delta t$  is the time shift between the two sensors  $S_1$  and  $S_2$ , the deviation of metering viscous liquid can be calculated based on water a benchmark,

$$Deviation = \frac{K_f \delta t_{viscous\ liquid} - K_f \delta t_{water}}{K_f \delta t_{water}} \times 100\% = \frac{\delta t_{viscous\ liquid} - \delta t_{water}}{\delta t_{water}} \times 100\% \quad (10)$$

The simulation results have been plotted in Fig 4 for the relation between the metering deviation and Reynolds number  $Re = \rho Dv / \mu$ . It is found that when the flow is laminar or transient flow ( $Re \leq 4000$ ), the deviation is fluctuating, while the deviation will be comparably flat when the flow is turbulent.

It is known that fluid with different viscosity may have different damping factor (Kumar and Anklin 2011). When the oscillation of the structure domain experience damping during fluid flow, the driver have to excite additional force to compensate for the amplitude loss caused by the fluid's damping. Since the damping affects the natural frequency of the flow tube, the meter factor  $K_f$  changes, the change directly affects the mass flow rate. The effect of the reduction in natural frequency is caused by the interaction between the fluid and structure dynamics in the CMF. In the future compensation modeling, the damping effect shall be considered.

#### 4. CONCLUSION

In this paper, a computational fluid dynamics model of U-shape CMF was developed to investigate the performance of CMFs influenced by on-line viscosity. The simulation results were evaluated in terms of the natural frequency of the vibrating system and the corresponding time difference between the motions of the sensing points symmetrically located on the measuring tube. The simulations of water and viscous liquid were compared over flow rates spanning the laminar and turbulent regions. The effects of viscosity on CMFs' performance have been discussed in details. The findings in the simulations can be used for further compensation of deviation due to viscosity effects for oil and gas industry.

#### References

- Bobovnik, G., N. Mole, J. Kutin, B. Stok and I. Bajsic (2005). Coupled finite-volume/finite-element modelling of the straight-tube Coriolis flowmeter. *Journal of Fluids and Structures*, 20, pp. 785-800.
- Henry, M., M. Tombs, M. Duta, F. Zhou, R. Mercado, F. Kenyery, J. Shen, M. Morles, C. Garcia and R. Langansan (2006). Two-phase flow metering of heavy oil using a Coriolis mass flow meter: A case study. *Flow Meas. Instrum.*, 17, pp. 399-413.
- Kumar, V. and M. Anklin (2011). Numerical simulations of Coriolis flow meters for low Reynolds number flows. *Mapan*, 26, pp. 225-235.
- Mole, N., G. Bobovnik, J. Kutin, B. Stok and I. Bajsic (2008). An improved three-dimensional coupled fluid-structure model for Coriolis flowmeters. *Journal of Fluids and Structures*, 24, pp. 559-575.